Time evolution of colliding laser produced magnesium plasmas investigated using a pinhole camera

S. S. Harilal, C. V. Bindhu, and H.-J. Kunze[a)]
Institut fuer Experimentalphysik V, Ruhr-Universitaet Bochum, Universitaetsstrasse 150, D-44780 Bochum, Germany

(Received 16 August 2000; accepted for publication 14 February 2001)

Time resolved studies of colliding laser produced magnesium plasmas are performed using a pinhole camera. A ruby laser pulse is split into two beams using a movable glass wedge and focused onto a planar target or targets placed at 90° to each other. A gated pinhole camera provides an orthogonal view of the collision. Measurements with an aluminum filter allowed identification of soft x-ray production zones. A good interpenetration of the two plasmas was observed in the 90° target geometry, because of higher relative velocities, than in the case of laterally colliding plasmas. The appearance of the collision region depended strongly on the power density and on the separation of the foci on the target surfaces. © *2001 American Institute of Physics.*
[DOI: 10.1063/1.1362408]

I. INTRODUCTION

A laser produced plasma is transient in nature with characteristic parameters that evolve quickly and are heavily dependent on irradiation conditions such as incident laser intensity, laser wavelength, irradiation spot size, ambient gas composition, and ambient pressure.[1–4] There are several diagnostic techniques for characterizing a laser produced plasma and these include optical emission spectroscopy,[3,4] mass spectroscopy,[5,6] laser induced fluorescence (LIF),[7,8] Langmuir probe,[9,10] microwave and laser interferometry,[11] and Thomson scattering.[12] Fast photography and other imaging techniques add another dimension to ablation diagnostics by providing two dimensional (2D) snap shots of the three dimensional (3D) plume propagation.[13] This capability becomes essential for a hydrodynamic understanding of the plume propagation and reactive scattering.[14] Recently, LIF using a gated intensified charged coupled device was applied to understand how nanoparticles form and grow in pulsed laser ablated plumes.[15,16] Furthermore, Puretzky *et al.*[17] observed a peculiar sharpening of a biomolecule plume during similar LIF imaging studies. However, most of the earlier reports concern fast photography of laser produced plasmas at times >50 ns and in the visible spectral region.[18,19] But at earlier times (<50 ns), most of the radiation emitted by a laser produced plasma source is in the x-ray, soft x-ray and extreme ultraviolet (XUV) region. Thus, a XUV photographic technique would be a versatile tool for studying the hydrodynamics of the plume at earlier times.

Several applications of laser produced plasmas involve an experimental situation where a plasma collision occurs. The understanding of the collision and subsequent interaction of the colliding plasmas is important, for example, for the design of inertial confinement fusion hohlraums.[20] Moreover, the subject of colliding and interpenetrating plasmas has attracted research directed toward achieving suitable conditions for x-ray amplification or directed x-ray transport.[21–23] Different target geometries are proposed in order to achieve suitable conditions for x-ray amplification in a laser produced plasma.[24] When two plasmas collide, various interactions may arise. These may be collisionless types in which collective plasma effects occur or collision dominated types. There are a variety of experimental configurations to explore the different types. Previous experiments have incorporated a variety of beam–target configurations including dual beam/parallel planar targets,[25] split beam/single planar target,[26] split beam/target slabs placed orthogonally,[22] and single beam/internally irradiated microtubes.[27] Very little has been done to image the spatial and temporal progression of colliding laser produced plasmas at very early times and especially in the XUV region. In this article, we report an experimental approach in which a gated XUV camera is used to image the expansion dynamics of colliding laser produced magnesium plasmas in vacuum. To understand and characterize the evolution of laterally and orthogonally colliding laser produced magnesium plasmas, charge coupled device (CCD) imaging was performed at different times after the laser vaporization pulse.

II. EXPERIMENTAL SETUP

A pulse from a ruby laser (6 J, 15 ns) was split into two beams using a movable glass wedge [Fig. 1(a)]. The position of the wedge was used to vary the intensity ratio of the two beams. We employed two experimental schemes for the target geometry. For producing laterally colliding plasmas, the laser beams are focused onto adjacent spots on a magnesium target slab and the two plasmas thus produced collide laterally [Fig. 1(b)]. We also employed another scheme where the two beams are focused onto two magnesium slabs placed 90° to each other [Fig. 1(c)]. In both cases, the target was kept in a vacuum chamber where the pressure was less than 10^{-5} Torr. The laser beams were focused onto the target surface using a planoconvex lens with a focal length, $f=300$ mm.

a)Electronic mail: hans-joachim.kunze@ep5.ruhr-uni-bochum.de

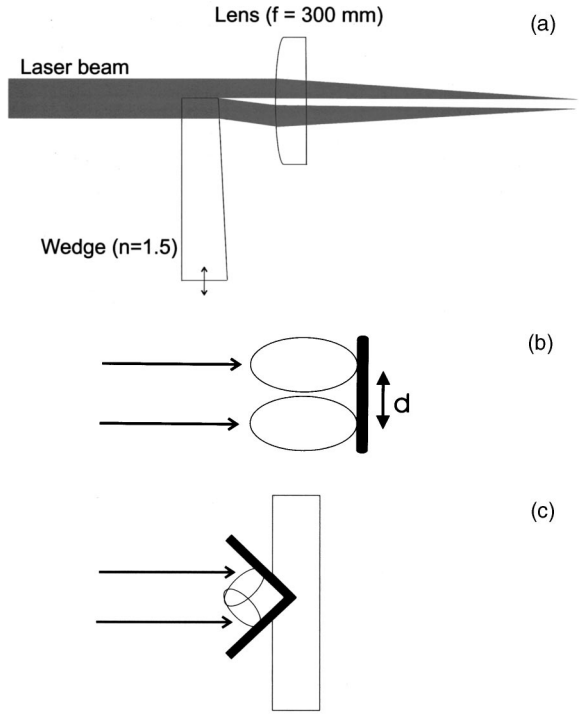

FIG. 1. (a) Schematic diagram of the wedge and lens combination used for splitting the laser beam (a), target geometry for laterally colliding plasmas (b), and target geometry for orthogonally colliding plasmas (c).

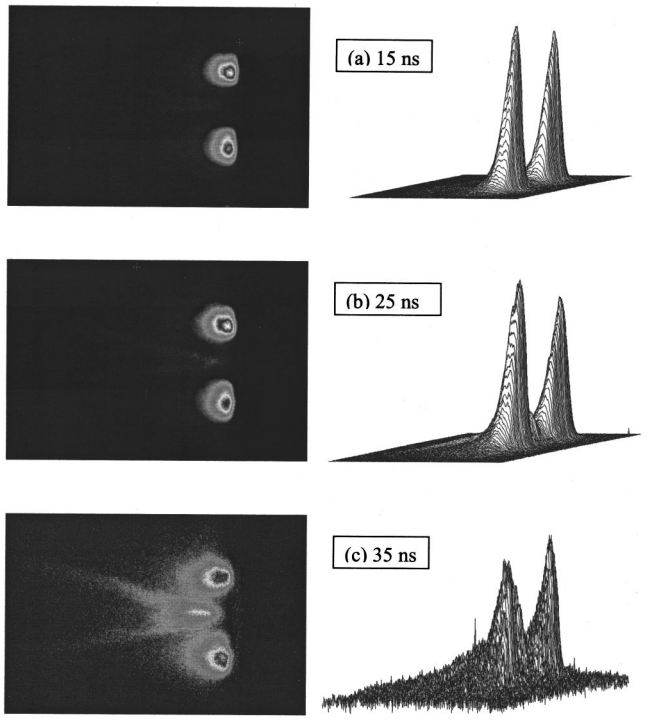

FIG. 2. Pinhole pictures of laterally colliding plasmas and their 3D intensity plots. The foci were separated by a distance of 0.75 mm. The time given in the pictures is the delay of the gate pulse after the laser pulse maximum. The gate was set to 5 ns.

The target slabs were placed on a motorized linear mount to translate the target after each shot. This prevented the creation of craters that tend to occlude emission from the hot core of the plasma. The distance between the two foci at the target surface is given by the relation

$$d = f\gamma(n-1), \tag{1}$$

where $n=1.5$ is the refractive index and γ is the acute angle of the wedge. In the present studies we used glass wedges with acute angles of $17'\ 02''$ and $34'\ 59''$ which corresponded to a distance of separation between the foci of $d=0.75$ mm and 1.5 mm, respectively. A gated (5 ns gate width) pinhole camera was used to record images of the colliding plasmas. The camera comprised a 50 μm pinhole and a microchannel plate (MCP) combined with a CCD. The camera also had an aluminum filter (27 μg cm^{-2}) which resulted in a spectral sensitivity for $\lambda < 80$ nm.

III. RESULTS AND DISCUSSION

The camera was installed to take pictures in a direction perpendicular to the plane of the two laser beams. The intensity ratio of the laser beams was made 1:1 and resulted in power densities of 1.3×10^{11} W cm^{-2} at both focal points. The camera was placed 5 cm away from the plane of the laser spots. The MCP/CCD was placed 45 cm from the pinhole and resulted in a magnification of nine at the CCD plane.

For producing laterally colliding plasmas, the two laser beams were focussed onto adjacent spots separated by a distance of 0.75 mm. The resulting plasmas expand away from the target but stream into each other in a direction parallel to the target surface. Figure 2 gives typical pinhole pictures of laterally colliding magnesium plasmas in 2D gray scale and 3D intensity plots. Rumsby *et al.*[28] studied the characteristics of laterally colliding plasmas using visible spectroscopy, but with this technique, it is rather difficult to study the dynamics at early times in the plasma expansion. Conversely, XUV pinhole pictures of plasmas reveal far more details about the expansion dynamics of the plasma plume at early times as XUV radiation is only emitted by a hot and dense plasma where higher ionization stages dominate, i.e., a plasma plume in its earliest stages.

The images taken at different times mirror the temporal displacement of the plume front and hence give the velocity of the plume. The expansion velocities of the plasmas were measured from the time evolution of the pinhole pictures and the estimated velocities of the plasmas in the initial stages are 4×10^6 cm s^{-1} in the Z direction (normal to the target surface) and 1.6×10^6 cm s^{-1} in the Y direction (lateral). Furthermore, the XUV plume length in a ns laser ablated plasma is limited to within 2 mm from the target surface and to less than 100 ns lifetime compared to a 5–6 cm plume length and a tens of microseconds of lifetime observed in the visible spectral region.[14]

Hitherto, the salient feature observed, during laterally colliding plasma investigations was that the plasmas do not merge and decay in a simple manner. Instead, now a dramatic configurational transformation is observed during which the emission of radiation is recorded. An interaction region is observed between the two plasma plumes at times greater than 14 ns. Another striking observation is that this interaction region is dense and hotter nearer to the target

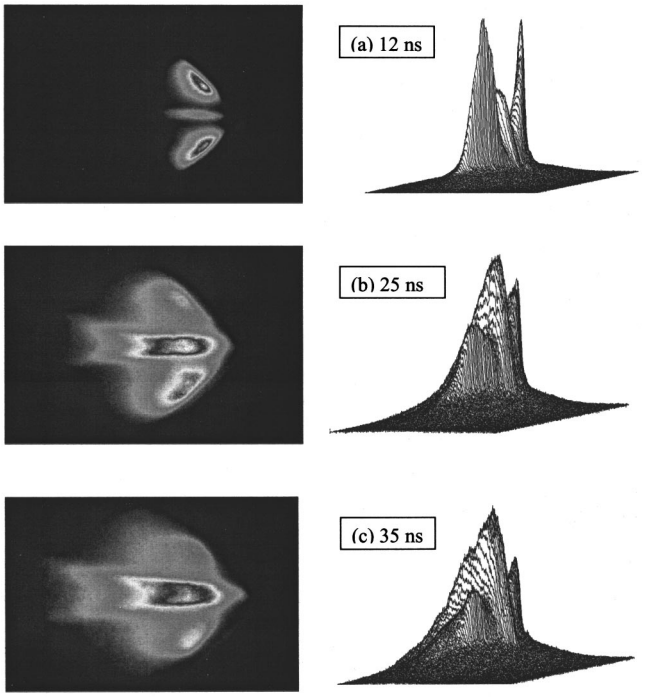

FIG. 3. Temporal evolution of colliding laser produced magnesium plasmas when the targets were placed 90° to each other. The right sides of the pinhole pictures represent their corresponding 3D intensity plots. At later times, the intensity of the colliding region is higher than that of the single plasmas. The foci were separated by a distance of 0.75 mm.

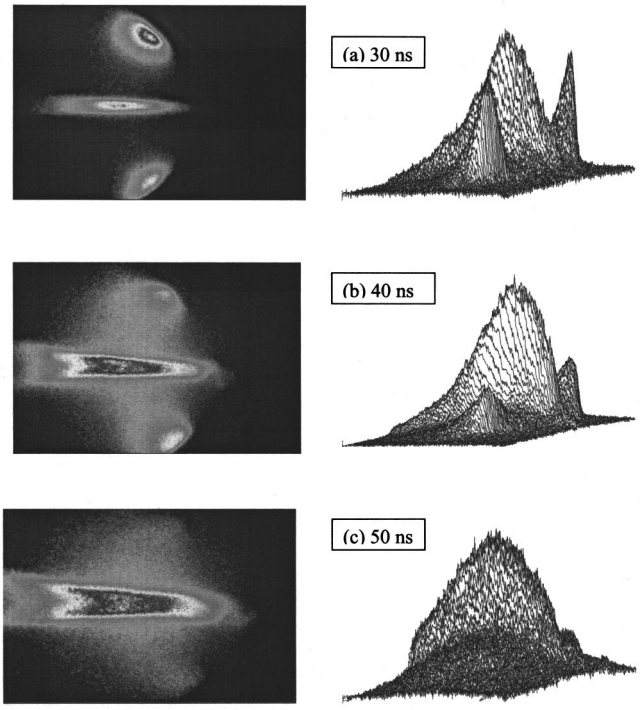

FIG. 4. Temporal evolution of colliding laser produced magnesium plasmas when the targets were placed 90° to each other and the foci were separated by 1.5 mm. The right sides of the pinhole pictures represent their corresponding 3D intensity plots. At later times, the intensity of the interaction region is higher than that of the single plasmas. The length and width of the interaction region is found to be higher in this case than with a foci separation of 0.75 mm.

surface and tail-like features begin to appear at larger distances from the target surface, which are directed sideways. The observation of such splitting of the interaction region at these distances can be due to lower densities of the plasmas in outer regions. It is also observed that the appearance of the interaction region is delayed with increasing separation of the foci. This is due to the longer time needed by the plasma species to interact with each other.

We also repeated the experiments with the targets mounted at an angle of 90° to each other. The arrangement led to a good interpenetration of the two plasmas because of the higher relative velocities than in the case of laterally colliding plasmas. The positions of the foci on the target surfaces were important parameters and governed the relative velocity with which the plasmas collided. In the present case, however, both the foci were located approximately equidistant from the common edge of the target surfaces and ensured a symmetric interaction region. It should be noted that slight changes in the geometry did cause drastic changes in the shape and position of the interaction region. Figure 3 represents time resolved pinhole pictures of the colliding plasmas using this 90° target geometry for a foci separation of 0.75 mm. Initially both plasmas expand freely, but as time evolves, a thin interaction region (about 75 μm) begins to evolve at the collision region and the intensity of the interaction region becomes brighter with time. It is interesting to note that the thickness of the interaction region becomes wider as time elapses. The length of the interaction region becomes $\sim$1 mm (including penumbral image) 15 ns after the laser pulse maximum. With the present 90° target geometry, the interaction region was found to appear at earlier times compared to the laterally colliding plasmas because of higher relative velocities.

Experiments were also performed with a foci separation of 1.5 mm. Figure 4 shows the time evolution of such plasmas in 2D gray scale and 3D intensity plots. In this case, the collision region is observed at later times in comparison with the 0.75 mm separation of the foci because of increased transit time. The pinhole pictures show an emission zone which appears like a jet starting in the collision region. There are only a few reports which describe the jet-like formation in laser produced plasma experiments. Farley *et al.*[29] produced a high Mach number, radiatively cooled jet using laser irradiation of a gold cone. They described that these radiative jets are similar to astrophysical jets in Mach number and cooling parameter, but not well matched in density contrast. Kodama *et al.*[30] studied specularly reflected light effects on the interaction of laser light with long length-scale plasmas and they observed a jet-like x-ray emission a few millimeters in length and in the direction of the specularly reflected light. In both the experiments described, they used laser power densities $>10^{15}$ W cm^{-2}. It should be noted that power densities in the present investigation are $\sim 10^{11}$ W cm^{-2}.

The spatial and temporal properties of this jet-like emission depended strongly on the laser power densities at the foci and on the position of the spots from the point of contact of the target surfaces.[31] The lifetime of the interaction region was found to be greater than the lifetime of the primary plasmas. The overall intensity of the colliding plasma was

found to increase with time and at long times the intensity of the collision region was higher than that of the single plasmas (see 3D intensity plots). For sufficiently low plasma densities where the ion–ion mean free path exceeds the dimensions of the system, the two plasmas interpenetrate with little collisional interaction. Interpenetration of the plasmas takes place at short times (<1 ns) and during this event the population density is perturbed by charge exchange collisions. At high plasma densities, where the ion–ion mean free path is smaller than the plasma density scale lengths, the region of plasma interpenetrating is relatively small. In this case, the plasma stagnates. The case of colliding plasmas with a low relative velocity is characterized by a wide heating region building up at later times, as observed with the laterally colliding plasmas (Fig. 2). Figures 3 and 4 illustrate the case of high velocity and high density, where the plasmas almost immediately stop after collision.

IV. CONCLUSIONS

XUV pinhole pictures of colliding laser produced magnesium plasmas are recorded at different times and thus characterize the plasma dynamics. An aluminum filter limited the observed radiation to wavelengths below <80 nm, i.e., to the soft x-ray and XUV region, and consequently the images only show the hot plasma region. Two target geometries were employed to investigate the nature of the colliding region. A good interpenetration of the two plasmas was observed with a 90° target geometry because of higher relative velocities than in the case of laterally colliding plasmas. The appearance of the collision region depends strongly on the power density and on the separation of the foci on the target surfaces. The collision region appears like a jet when the targets are 90° to each other. When one plasma collides with another plasma the directed kinetic energy can be converted into thermal energy and the plasma heats up and slows down. This forms a plasma which is nearly stationary but has the appearance of a jet.

ACKNOWLEDGMENT

One of the authors (S.S.H.) thanks the Alexander von Humboldt Foundation, Germany for a research fellowship.

[1] W. L. Kruer, Phys. Plasmas **7**, 2270 (2000).
[2] D. H. Lowndes, D. B. Geohegan, A. A. Puretzky, D. P. Norton, and C. M. Rouleau, Science **273**, 898 (1996).
[3] S. S. Harilal, C. V. Bindhu, V. P. N. Nampoori, and C. P. G. Vallabhan, Appl. Phys. Lett. **72**, 167 (1998).
[4] S. S. Harilal, C. B. Bindhu, V. P. N. Nampoori, and C. P. G. Vallabhan, J. Appl. Phys. **82**, 2140 (1997).
[5] S. M. Park and J. Y. Moon, J. Chem. Phys. **109**, 8124 (1998).
[6] C. P. Safvan, F. A. Rajgara, V. Bhardwaj, G. R. Kumar, and D. Mathur, Chem. Phys. Lett. **255**, 25 (1996).
[7] A. A. Puretzky and D. B. Geohegan, Appl. Surf. Sci. **127**, 248 (1998).
[8] Y. Nakata, H. Kaibara, T. Okada, and M. Maeda, J. Appl. Phys. **80**, 2458 (1996).
[9] B. Toftmann, J. Schou, T. N. Hansen, and J. G. Lunney, Phys. Rev. Lett. **84**, 3998 (2000).
[10] R. M. Mayo, J. W. Newman, A. Sharma, Y. Yamagata, and J. Narayan, J. Appl. Phys. **86**, 2865 (1999).
[11] H. Shcittenhelm, G. Callies, P. Berger, and H. Hugel, Appl. Surf. Sci. **129**, 922 (1998).
[12] R. C. Elton, J. A. Cobble, H. R. Griem, D. S. Montgomery, R. C. Mancini, V. L. Jacobs, and E. Behar, J. Quant. Spectrosc. Radiat. Transf. **65**, 185 (2000).
[13] S. S. Harilal, C. V. Bindhu, and H.-J. Kunze, J. Phys. D **34**, 560 (2001).
[14] B. Angleraud, J. Aubreton, and A. Catherinot, Eur. Phys. J.: Appl. Phys. **5**, 303 (1999).
[15] A. A. Puretzky, D. B. Geohegan, X. Fan, and S. J. Pennycook, Appl. Phys. A: Mater. Sci. Process. **70**, 153 (2000).
[16] D. B. Geohegan, A. A. Puretzky, and D. J. Rader, Appl. Phys. Lett. **74**, 3788 (1999).
[17] A. A. Puretzky, D. B. Geohegan, G. B. Hurst, M. V. Buchanan, and B. S. Luk'yanchuk, Phys. Rev. Lett. **83**, 444 (1999).
[18] A. Misra and R. K. Thareja, IEEE Trans. Plasma Sci. **27**, 1553 (1999).
[19] F. Kokai, K. Takahashi, K. Shimizu, M. Yudasaka, and S. Iijima, Appl. Phys. A: Mater. Sci. Process. **69**, S223 (1999).
[20] T. R. Dittrich, S. W. Haan, M. M. Marinak, S. M. Pollaine, D. E. Hinkel, D. H. Munro, C. P. Verdon, G. L. Strobel, R. McEachern, R. C. Cook, C. C. Roberts, D. C. Wilson, P. A. Bradley, L. R. Foreman, and W. S. Varnum, Phys. Plasmas **6**, 2164 (1999).
[21] H.-J. Kunze, K. N. Koshelev, C. Steden, D. Uskov, and H. T. Wieschebrink, Phys. Lett. A **193**, 183 (1994).
[22] F. Ruhl, L. Aschke, and H. J. Kunze, Phys. Lett. A **225**, 107 (1997).
[23] R. W. Clark, J. Davis, A. L. Velikovich, and K. G. Whitney, Phys. Plasmas **4**, 3718 (1997).
[24] D. Vick, M. Kado, H. Yamamoto, A. Nishiguchi, K. A. Tanaka, K. Mima, A. A. Offenberger, C. E. Capjack, and S. Nakai, Phys. Rev. E **48**, 2308 (1993).
[25] R. A. Bosch, R. L. Berger, B. H. Failor, N. D. Delamater, G. Charatis, and R. L. Kauffman, Phys. Fluids B **4**, 979 (1992).
[26] V. Henc-Bartolic, Z. Andreic, D. Gracin, L. Aschke, F. Ruhl, and H. J. Kunze, Phys. Scr., T **75**, 297 (1998).
[27] C. Stockl and G. D. Tsakiris, Laser Part. Beams **9**, 725 (1991).
[28] P. T. Rumsby, J. W. M. Paul, and M. M. Masoud, Phys. Plasmas **16**, 969 (1974).
[29] D. R. Farley, K. G. Estabrook, S. G. Glendinning, S. H. Glenzer, B. A. Remington, K. Shigemori, J. M. Stone, R. J. Wallace, G. B. Zimmerman, and J. A. Harte, Phys. Rev. Lett. **83**, 1982 (1999).
[30] R. Kodama, K. A. Tanaka, Y. Sentoku, T. Matushita, K. Takahashi, H. Fujita, Y. Kitagawa, Y. Kato, T. Yamanaka, and K. Mima, Phys. Rev. Lett. **84**, 674 (2000).
[31] S. S. Harilal, C. V. Bindhu, and H.-J. Kunze, Proceedings of the Ultraintense Laser Matter Interactions and Applications, Euroconferences Pisa, Italy, p. 120.